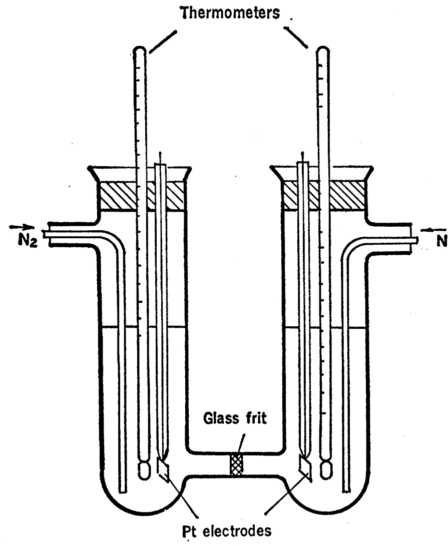

Fig. 1. Schematic drawing of the experimental cell.

$(CN)_8 \cdot 8H_2O$," and finally to "$K_4Mo(CN)_8 \cdot 8H_2O$" (*1*, pp. 410–413). In parallel, the same preparative route to "$K_4Mo(CN)_8 \cdot 8H_2O$" was followed, starting with a concentrated HCl solution of "$MoCl_4$" (Research Organic/Inorganic Chemical Corporation, Sun Valley, California). The polarograms of the two substances were identical, showing a half-wave potential $E_{1/2}$ of −0.12 volt.

The formation of Mo^{5+} on the illuminated side of the cell was established as follows: The brown precipitate formed upon irradiation was dissolved in HCl and reprecipitated with ammonium carbonate as brown "$MoO(OH)_3$" (*1*, pp. 406–407). The polarogram of this substance in 3*N* HCl was identical with a polarogram obtained from a sample of "$MoO(OH)_3$" prepared by adding ammonium carbonate to a concentrated HCl solution of "$MoCl_5$" (Research Organic/Inorganic Chemical Corporation). Both samples show polarograms with half-wave potentials of −0.11 volt and −0.45 volt.

That Mo^{3+} was formed in the dark side of the cell was shown by comparing the polarogram of a known sample of "$(NH_4)_2MoCl_5 \cdot H_2O$" with that of the dark red precipitate obtained by adding ammonium carbonate to the solution in the dark side (*1*, pp. 413–415). The polarograms of these two materials were identical ($E_{1/2} = -0.43$ volt).

The concepts that we applied to identify the present photovoltaic liquid were the following:

1) Ions, atoms, and molecules all become stronger reducing agents upon excitation: The electron promoted to a higher energy level requires less energy for its removal.

2) To obtain efficient electron transfer reactions it is necessary to have relatively long-lived excited states. If either the radiationless or the radiative transitions are excessively rapid relative to the electron transfer reaction, the quantum yields are small and the effects negligible. Criteria for adequately long life are (i) photochemical reactivity of the excited species and (ii) luminescence with long decay. Molybdenum (IV) is known to undergo photochemical reactions, and photoelectron ejection has been reported in the cyano complex of Mo^{4+} (*2*).

3) The absorption spectrum of the product in the illuminated cell must not mask the spectrum of the reactant. The Mo^{4+} ion is deep green; the product (the Mo^{5+} formed in the illuminated side) is light brown and precipitates out.

4) The rate of reverse reaction, in which the photooxidized species is reduced by the ejected solvated electron, or by a reduced material that is produced, must be slow relative to the diffusion of the solvated electron to the electrode or the diffusion of the reduced intermediary to the electrode. This criterion is met in our experiment because the solubility of Mo^{5+} in our solution at *p*H 4 is limited and the oxidized product is removed from the equilibrium when formed. Indeed, our photovoltaic cell cannot be operated in strongly acid solutions, in which Mo^{5+} dissolves.

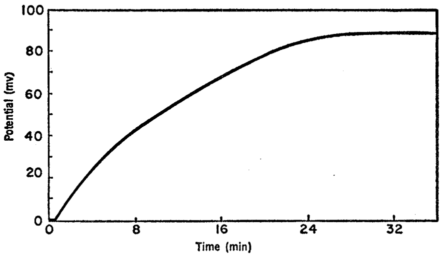

Fig. 2. Development of the potential after exposure of the half-cell to light.

MARJORIE H. NAVIDI
HARRY G. BRITTAIN
Chemistry Department, Queens College, City University of New York, Flushing 11367
ADAM HELLER
Bayside Research Center of General Telephone & Electronics Laboratories, Inc., Bayside, New York 11360

References

1. W. G. Palmer, *Experimental Inorganic Chemistry* (Cambridge Univ. Press, London, 1965).
2. W. L. Waltz, A. W. Adamson, P. D. Fleischaver, *J. Amer. Chem. Soc.* **89**, 3923 (1967).

5 June 1970; revised 2 July 1970

Garnet: First Occurrence in the Lunar Rocks

Abstract. *Three grains of almandine-rich garnet isolated from lunar sample 12021 have the composition $Alm_{70.7}Gro_{25.0}Sp_{2.7}Pyr_{1.6}$, with cell edge of 11.624 angstroms and refractive index of 1.81. The garnet probably formed late in the crystallization sequence.*

In our study of lunar sample 12021 returned by the Apollo 12 mission, we have identified three grains of garnet. This rock was described by the Lunar Sample Preliminary Examination Team (*1*) as a porphyritic gabbro, and we have examined a small rock chip (12021,22) and a polished thin section (12021,2). The rock chip, wrapped in aluminum foil, was partly disaggregated when received, and the enclosing foil contained several hundred mineral and rock fragments ranging in size from a few micrometers to a millimeter. During examination of the fragmental material under a binocular microscope, three distinctive grains were observed and isolated (*2*). These grains were pale brown in color with a distinct pink tinge and were free from inclusions, having a gem-quality appearance. They were anhedral and somewhat flattened, varying from 100 to 300 μm in the largest dimension and averaging less than 40 μm in thickness.

The three grains were used for an x-ray powder pattern, microprobe analysis, and refractive index determination. The x-ray powder pattern (*3*) identified the grain as garnet, with a cell edge of 11.624 ± 0.005 Å. The electron microprobe analysis (*4*) showed that the garnet is rich in iron and calcium, with minor amounts of manganese and magnesium (see Table 1). No evidence of chemical zoning was detected in this grain. In calculating the atomic formula (Table 1), all of the iron is assumed to be divalent. This assumption is reasonable in view of the highly re-

Table 1. Electron microprobe analysis and atomic formula on the basis of 12 oxygens for garnet grains from lunar sample 12021,22. The following elements were not detected: Cr, Y, K, and Na.

Chemical analysis		Atomic proportions		
SiO_2	36.1	Si	2.938	3.000
TiO_2	0.1	Al	0.052	
Al_2O_3	21.4	Al	1.991	1.997
FeO	31.5	Ti	0.006	
MnO	1.2	Fe	2.144	3.033
MgO	0.4	Mn	0.083	
CaO	8.7	Mg	0.048	
		Ca	0.758	
Total	99.4			

duced conditions under which the Apollo 11 rocks crystallized (*5*) and which are considered to hold true for Apollo 12 rocks (*1*). Although it was not possible to measure the specific gravity of the grains, the refractive index of 1.81 (determined on the third grain) and the cell edge are in accord (*6*) with the microprobe analysis recalculated into end-member molecules (*7*): $\mathrm{Alm}_{70.7}\mathrm{Gro}_{25.0}\mathrm{Sp}_{2.7}\mathrm{Pyr}_{1.6}$.

Garnet has not so far been observed in contact with other minerals in the rock fragments, owing to its apparent rarity and color resemblance to the paler brown pyroxenes. Nor has it been observed in the thin section. We therefore have no direct evidence about its paragenesis or association. However, the anhedral form of the grains suggests that they occur interstitially rather than as phenocrysts or in vugs.

Garnets are a rare constituent of terrestrial igneous rocks (*8*) and, among 480 garnet analyses collected by Tröger (*9*), none is reported to occur in igneous rocks of basaltic composition. Almandine-rich garnets are found as phenocrysts in intermediate to felsic extrusives (*8*) and in cavities in felsic volcanics (*10*). It is of interest to note also that, for an almandine-rich garnet, the total almandine plus grossular content (95.7 mole percent) of the lunar garnet exceeds that of any terrestrial garnet reported by Tröger.

The presence of garnet in sample 12021 appears to be somewhat of an enigma. The gross mineral assemblage of this rock—spinels, ilmenite, pyroxenes, plagioclase, cristobalite, tridymite, troilite, native iron and minor pyroxferroite, alkali feldspar, and apatite—is very similar to some of the Apollo 11 crystalline rocks, and yet none of the investigators (see *Science*, 30 January 1970) reported garnet in these samples. Since garnet is obviously a rare mineral in sample 12021, it seems unlikely that differences in bulk rock composition are important; it would seem, instead, that some particular crystallization condition(s) permitted its formation. From our observations of section 12021,2, it would appear that the conditions under which the Apollo 11 crystalline rocks formed (very low oxygen fugacity and extreme crystal fractionation, with the consequent development of iron-enriched liquids) also hold true for this sample, as does the development of a felsic residuum as the end product. The iron-rich composition, the moderate calcium content, and the extremely low magnesium content, together with the relatively high manganese content for a lunar mineral and the absence of zoning, suggest that the garnet, like pyroxferroite, formed late in the crystallization sequence.

R. J. Traill
A. G. Plant
J. A. V. Douglas
Geological Survey of Canada, Department of Energy, Mines and Resources, Ottawa, Ontario, Canada

References and Notes

1. Lunar Sample Preliminary Examination Team, *Science* **167**, 1325 (1970).
2. Two gray-blue grains, less than 100 μm in size, were also isolated and have been identified as amphibole from the x-ray powder pattern. Further study of this mineral is in progress.
3. CuKα, 57.4-mm radius.
4. Anaiysis was obtained with a Materials Analysis Company model 400S electron microprobe at 20 kv and 0.03 μa specimen current using a chemically analyzed garnet as standard.
5. M. R. Dence, J. A. V. Douglas, A. G. Plant, R. J. Traill, *Geochim. Cosmochim. Acta* Suppl. **1 1**, 315 (1970).
6. H. Winchell, *Amer. Mineral.* **43**, 595 (1958).
7. The garnets comprise a group of isomorphous minerals having the general formula $X_3Y_2(SiO_4)_3$. Because of extensive atomic substitution, the composition is commonly expressed in terms of proportions of the following end-member molecular compositions:

Almandine	(Alm)	$Fe_3Al_2(SiO_4)_3$
Pyrope	(Pyr)	$Mg_3Al_2(SiO_4)_3$
Spessartine	(Sp)	$Mn_3Al_2(SiO_4)_3$
Grossular	(Gro)	$Ca_3Al_2(SiO_4)_3$
Andradite	(And)	$Ca_3Fe_2(SiO_4)_3$
Uvarovite	(Uv)	$Ca_3Cr_2(SiO_4)_3$

8. L. C. Hsu, *J. Petrol.* **9**, 40 (1968).
9. E. Tröger, *Neues Jahrb. Mineral. Abh.* **93**, 1 (1959).
10. R. L. Oliver, *Geol. Mag.* **93**, 121 (1956).
11. We thank M. Bonardi for measuring the x-ray pattern.

22 June 1970

■

Earth's Gravity Field: Relation to Global Tectonics

Abstract. *An improved solution for the gravity field shows ocean rises, as well as trench and island arcs, as mass excesses. Ocean basins, areas of recent glaciation, and the Asian portion of the Alpide belt are mass deficiencies. Most features appear interpretable as varying behavior of the lithosphere in response to asthenospheric flow.*

An improved determination of the gravity field from satellite orbits, supplemented by terrestrial gravimetry, has been made by Gaposhkin and Lambeck (*1*). The results are given in the form of spherical harmonic coefficients of the potential complete through the 16th degree, plus a few of higher degree; hence the resolution of the data is about 11°, or 1200 km.

The new gravity field is shown in Fig. 1 in the form of free-air gravity anomalies referred to the figure of hydrostatic equilibrium, an ellipsoid of flattening 1/299.8. Anomalies are preferable to the customary geoid heights because the shorter wavelength variations are not obliterated.

The one great consequence of the improved resolution is to break up the two largest features in the southern oceans that appeared in previous solutions (*2*). A large area of mild anomaly in the South Pacific is now resolved into two negative areas with a positive area between them; the negative areas are over basins and the positive area is along the East Pacific Rise. In the area between Africa and Antarctica, a single large positive feature centered in the "vee" between the two rises is now divided into two positive features over the rises and an area of mild anomaly between. Thus the great majority of ocean rises are now seen to be associated with positive anomalies, rather than being of mild anomaly, as inferred from older data. The new solution also shifts or modifies several other features whose correlation with tectonics has previously been puzzling (*2*).

As in earlier studies, the correlation of gravity with topography is poor for 5th and lower degrees, suggesting a deep-seated cause for this part of the field, such as that recently hypothesized by Hide and Malin (*3*). The gravity field residual to the 5th degree does, in fact, have significantly higher correlation of positive anomalies with ocean rises. This correlation is even more emphasized if isostatic, instead